DOI: 10.26599/FSHW.2025.9251029

Contents lists available at SciOpen

Food Science and Human Wellness

journal homepage: https://www.sciopen.com/journal/2097-0765

China Food Publishing Co.

Impact of aging on physicochemical properties of dried abalone and immunomodulatory activities of its simulated *in vitro* digestion products

Chuyu Xi[a], Linfan Shi[ab], Zhongyang Ren[ab], Wuyin Weng[a,b*]

[a]*College of Ocean Food and Biological Engineering, Jimei University, Xiamen 361021, China*

[b]*Fujian Provincial Engineering Technology Research Center of Marine Functional Food, Xiamen 361021, China*

ABSTRACT: During the long aging process of dried abalone not only are distinctive color, flavor, and texture developed, but the immunomodulatory potential of its protein-derived components may also be altered. Therefore, the physicochemical properties of dried abalone aged for 0, 3, 5, and 10 years were investigated, and the immunomodulatory activity of their mimic digestion products (MDP) were evaluated. The results demonstrated that during the aging process, a gradual decrease was observed in both lightness (L^*) and whiteness (W^*) values of dried abalone. Concurrently, the A_{294} and A_{420} values were increased from 0.53 to 0.93 and from 0.08 to 0.17, respectively, accompanied by a reduction in endogenous fluorescence intensity. SDS-PAGE analysis revealed that prolonged aging led to partial degradation of myofibrillar protein, with the simultaneous formation of high-molecular-weight aggregates. The proportion of oligopeptides below 1000 Da in MDP was elevated, among which glutamate was determined to be the most abundant amino acid. Regarding immunomodulation activity, 3-year-aged dried abalone MDP exhibited the most potent stimulation of RAW264.7 cell proliferation rate at 236.37%, whereas 0-year-aged dried abalone MDP elicited the strongest phagocytic activity at 42.79%. In contrast, 0-year-aged dried abalone MDP was shown to induce the highest secretion of 1.53 μM NO and 19.18 ng/mL TNF-α when administered alone. A synergistic effect was observed when 5-year-aged dried abalone MDP were co-administered with LPS, resulting in a remarkable increase of TNF-α from 45.50 to 122.89 ng/mL and IL-6 from 5.72 to 19.52 ng/mL. Furthermore, the combined application of 5-year-aged dried abalone MDP and LPS effectively upregulated the expression of CD80 from 7.41% to 94.22% and CD86 from 51.30% to 68.87%. These findings suggest that the aging process likely induces Maillard reactions in dried abalone, thereby potentiating the immune-activating properties of its digestion products.

Key words: dried abalone; aging duration; pepsin-trypsin mimic digestion; RAW264.7 cell; immunomodulatory activity

1. Introduction

The Japanese abalone (*Haliotis discus hannai* Ino), a marine gastropod mollusk of the family Haliotidae, is highly valued in East Asian culinary traditions and nutraceutical applications due to its exquisite taste and exceptional nutritional profile. As a premium "marine delicacy", it represents a valuable source of high-quality protein, crucial amino acids, and various bioactive compounds with demonstrated

***Corresponding author**
wwymail@jmu.edu.cn

Received 30 June 2025
Received in revised from 8 October 2025
Accepted 12 November 2025

health benefits, including antioxidant, anti-inflammatory, and antitumor activities[1]. Our previous research has established that abalone proteins, primarily composed of myofibrillar proteins and collagen, contribute significantly to both its nutritional profile and unique textural properties[2]. As the world's leading producer of farmed abalone, China achieved an annual output reaching 245,000 metric tons in 2023[3], with a substantial portion being processed into value-added products including dried abalone[4]. The dried abalone is considered a gourmet ingredient, with the prized "candy abalone" (Tangxin dried abalone) developing characteristic viscoelastic texture through specialized processing[5].

In the traditional processing of high-quality dried abalone, the products are typically subjected to an aging process lasting several years. The presence of salt and sugar in dried abalone can inhibit the growth of spillage microorganisms under cool and dry storage conditions. Moreover, the quality and flavor of dried abalone are further improved with prolonged aging, leading to an increase in its market value. This process is accompanied by non-enzymatic browning reactions and protein structural modifications, thereby inducing a series of complex physicochemical transformations[6,7]. It is reported that Maillard reaction products can exert the immunomodulatory function of RAW264.7 cells after *in vitro* digestion[8]. Although the immunomodulatory activities of abalone polysaccharides have been well-documented in a prior study[9], the bioactive potential of mimic digestion products from aged dried abalone, particularly their immunomodulatory effects, remains unexplored. The aging is known to influence the texture and flavor quality of dried abalone, but its specific impact on the immunomodulatory activity of the protein-derived components is poorly characterized. Current research on immunomodulation of abalones has primarily focused on fresh meat or processing by products[10], yet growing evidence suggests that various food protein hydrolysates possess immunomodulatory potential[11,12]. Therefore, the influence of aging duration on the immunomodulatory activity of digested dried abalone products should be investigated.

This study was designed to investigate the relationship between natural aging duration and immunomodulatory activity of pepsin-trypsin mimic digestion products (MDP) from dried abalone. Commercially available dried abalone samples aged for 0, 3, 5, and 10 years were selected as research subjects. The physicochemical properties of dried abalone with different aging duration were analyzed, and the immunomodulatory activities of their corresponding MDP were evaluated. Unlike short-term storage studies conducted under accelerated conditions such as 40 °C[6], the samples used in this study were all commercial products, with aging process occurred naturally over years in actual storage and distribution environments, thus better reflecting the true quality of commercial products. This experimental design helps reveal the changes patterns in immunoregulatory activity during the long-term natural aging of dried abalone under realistic conditions. The findings of this study are expected to provide scientific reference for enhancing consume understanding of the functional nutritional value of aged dried abalone.

2. Material and methods

2.1. Materials and chemicals

The dried abalone samples (*Haliotis discus hannai* Ino) with different aging periods (0-year-aged: ~ 45.00 g/individual; 3-year-aged: ~ 67.00 g/individual; 5-year-aged: ~ 32.00 g/individual; 10-year-aged: ~ 28.00 g/individual) were purchased from Haolin (Guangzhou) Food Trading Co., Ltd. All dried abalone samples were prepared using uniform drying process from *Haliotis discus hannai* Ino raw materials. The 3-year-aged dried abalone, produced during the COVID-19 pandemic, are generally larger than that from other years due to the prolonged cultivation period.

Pepsin and trypsin were purchased from Aladdin Reagent (Shanghai) Co., Ltd. (Shanghai, China). Limulus Amebocyte Lysate Chromogenic Assay Kit was purchased from Xiamen Bioendo Technology Co., Ltd. (Fujian, China). HPLC-grade acetonitrile, trifluoroacetic acid and methanol were purchased from Merck KGaA (Darmstadt, Germany). HPLC-grade O-phthaldialdehyde (OPA) and 9-fluorenylmethyl chloroformate (FMOC) were purchased from Agilent Technologies Inc. (California, USA). DMEM high-glucose medium, phosphate buffer saline (PBS) and Lipopolysaccharide (LPS) were purchased from Labgic Technology Co., Ltd. (Beijing, China). 10% heat-inactivated fetal bovine serum was purchased from Biological Industries Israel Beit Haemek, Ltd. (Kibbutz Beit-Haemek, Israel). 1% penicillin-streptomycin and CCK-8 assay were purchased from Beijing Solarbio Science and Technology Co., Ltd. (Beijing, China). FITC-labeled 40 kDa dextran was purchased from Shanghai Maokang Biotechnology Co., Ltd. (Shanghai, China). Nitric oxide test kit was purchased from Beyotime Biotechnology Co., Ltd. (Shanghai, China). QuantiCyto® Mouse TNF-α ELISA kit and QuantiCyto® Mouse IL-6 ELISA kit were purchased from Shenzhen NeoBioscience Technology Co., Ltd. (Guangdong, China). FITC Plus Anti-Mouse CD80 (B7-1) (16-10A1) and FITC Plus Anti-Mouse CD86 (GL1) were purchased from Proteintech Group, Inc. (Illinois, USA). Flow cytometry staining buffer (FACS buffer) was purchased from MultiSciences (Lianke) Biotech Co., Ltd. (Zhejiang, China). All other chemicals and solvents were of analytical grade.

2.2. Sample preparation

The dried abalone samples were sliced into small pieces using a sterilized cleaver. The obtained slices were ground into powder using liquid nitrogen. The resulting dried abalone powder was divided into aliquots and stored at -20 °C until analysis.

2.3. SDS-PAGE

The dried abalone powder dissolved in a denaturing buffer (8.00 mol/L urea, 2% (w/v) SDS, 20.00 mmol/L Tris-HCl, pH 8.80). SDS-PAGE was performed according to the method of Laemmli[13] using a discontinuous gel system consisting of a 4% stacking gel and an 8% separating gel. Electrophoresis was run at 8.00 mA constant current. After electrophoretic separation, the protein bands were visualized using Coomassie Brilliant Blue R-250 staining, followed by destaining with a methanol/acetic acid/water solution (3:1:6, v/v/v). Protein bands were visualized and documented.

2.4. Color

The color analysis was determined according to the method of Luo et al.[14] with modifications. Color analysis was performed using a color photometer (YS3010, 3nh Technology, Shenzhen, Guangdong, China). The following color parameters were measured: L^* (lightness), a^* (redness/greenness) and b^* (yellowness/blueness). Before measurement, sample (3.00 g) was evenly spread in a measurement dish (diameter: 3.00 cm) to ensure consistent thickness and surface smoothness. The color photometer was calibrated using a white standard reference. Each sample was analyzed in six replicates. The W^* (whiteness) was calculated by Equation (1):

$$W^*=100-[(100-L^*)^2+a^{*2}+b^{*2}]^{1/2} \quad (1)$$

2.5. Browning index

The browning index was determined according to the method of Luo et al.[6] with modifications. Samples were dissolved in the same denaturing buffer as described in Section 2.3. For measurement, 2.00 mL of sample solution (5.00 mg/mL) was analyzed using an ultraviolet spectrophotometer (UV-8000A, Yuanxi Instrument, Shanghai, China), with absorbance readings taken at 294 nm and 420 nm. Each sample was analyzed in six replicates.

2.6. Intrinsic fluorescence spectra

The intrinsic fluorescence characteristics were analyzed according to the method described by Qiu et al.[15] with modification. The samples were dissolved in the same denaturing buffer as described in Section 2.3 and adjusted to final concentration of 2.5 mg/mL. Fluorescence spectra were performed on a fluorescence spectrophotometer (Cary Eclipse, Agilent, Santa Clara, California, USA) with the following settings: scan speed of 600 nm/min, excitation wavelength of 295 nm, and emission wavelength range of 300-600 nm. Each sample (5.00 mg/mL, 2.00 mL) was analyzed in triplicate.

2.7. Preparation of pepsin-trypsin mimic digestion products (MDP)

Gastrointestinal digests of dried abalone were prepared according to an optimized sequential enzymatic protocol. Briefly, 1.00 g of sample powder was homogenized with 10.00 mL distilled water in an ice bath using a high-speed homogenizer (FA25 model, FLUKO, Shanghai, China). The homogenate was adjusted to pH 2.00 with 1.00 mol/L HCl, then mixed with 1.00 mL pepsin solution (30.00 mg/mL) for gastric digestion (37 °C, 150 rpm, 2 h). The reaction was terminated by adjusting pH to 7.00 using 1.00 mol/L NaOH, followed by further adjustment to pH 7.50 for intestinal digestion with 1.00 mL trypsin solution (40.00 mg/mL) under the same conditions (37 °C, 150 rpm, 2 h). Enzymatic reactions were completely inactivated by heating at 100 °C-water bath for 5 min. The hydrolysates were precipitated with 3.00 mL anhydrous ethanol at 4 °C for 12 h, centrifuged at 10,000 × *g* for 20 min at 4 °C, and the supernatant was lyophilized and stored at -20 °C. All prepared samples were confirmed to be endotoxin-free (< 0.1 EU/mL) using the Limulus Amebocyte Lysate chromogenic assay.

2.8. Molecular weight distribution

Molecular weight distribution of MDP was performed on an Agilent 1200 high-performance liquid chromatography (HPLC) system (Santa Clara, California, USA) with a Tosoh TSK-G2000 SWXL column (300 mm × 7.8 mm) (Tokyo, Japan) according to the method of Weng et al.[16]. The mobile phase (45% acetonitrile, 55% water, and 0.10% TFA) flowed at 0.50 mL/min with detection at 214 nm. With the column stabilized at 25 °C, samples were injected at a volume of 20.00 μL. Calibration was performed using standard peptides (1-5 kDa). Each sample was analyzed in triplicate.

2.9. Amino acid composition

Amino acid composition of MDP was determined according to the method of Weng et al.[16] with modifications. Samples (0.01 g) were hydrolyzed with 6.00 mol/L HCl in nitrogen-flushed tubes (110 °C, 22 h). After HCl removal by rotary evaporation, hydrolysates were reconstituted in 2.00 mL 20.00 mmol/L HCl, filtered through 0.22 μm membranes, and derivatized with OPA and FMOC reagents. Analysis was performed on an Agilent 1200 HPLC system (Santa Clara, California, USA) with a ZORBAX Eclipse AAA column (4.6 × 150 mm, 3.50 μm) (Agilent, Santa Clara, California, USA) at 40 °C. The mobile phases system was consisted of two eluents: (A) 40.00 mmol/L Na_2HPO_4 (pH 7.8) and (B) a ternary mixture of acetonitrile/methanol/water (45:45:10, v/v/v), delivered at a flow rate of 1.00 mL/min. Detection was performed at 338 nm for primary amino acids followed by 262 nm for secondary amino acids. Calibration used standard amino acid mixtures with triplicate measurements per sample.

2.10. Cell culture

The murine RAW264.7 macrophage cell line was obtained from the research group of Professor Lingyan Su at Yunnan Agricultural University as a generous gift, and cultured in high-glucose DMEM containing 10% heat-inactivated fetal bovine serum (FBS) and 1% penicillin-streptomycin. The cells were maintained at 37 °C in a humidified 5% CO_2 incubator (Thermo Scientific, Thermo Fisher Scientific Inc., Waltham, Massachusetts, USA). Upon reaching 80% confluence, they were passaged at a 1:3 ratio, and only cells in the logarithmic growth phase (below passage 20) were utilized for experiments.

2.11. Cell viability assay

Cell viability and proliferation were assessed using the CCK-8 assay. Cell suspensions (1.00×10^5 cells/mL) were plated in 96-well plates and allowed to adhere for 24 h before exposure to MDP at concentrations ranging from 0 to 12.80 mg/mL for 24 h. Following treatment, 10.00 μL of CCK-8 reagent was added to each well, and after 2 h of incubation at 37 °C, optical density (OD) was determined at 450 nm using a microplate reader (BioTek, Winooski, Vermont, USA). Cell viability was calculated by Equation (2):

$$\text{Cell viability (\%)} = \left(\frac{A_{Experimental} - A_{Blank}}{A_{Control} - A_{Blank}}\right) \times 100 \quad (2)$$

where $A_{Experimental}$ is the OD_{450} of the experimental well; A_{Blank} is the OD_{450} of the blank well (background control); $A_{Control}$ is the OD_{450} of the untreated control well.

2.12. MDP-induced differentiation of RAW264.7 cells

Confluent RAW264.7 cells (~ 80%) were plated in 6-well plates (1.00×10^5 cells/mL, 2.00 mL/well). Following overnight culture, cells were treated with (1) MDP (0 - 6.40 mg/mL); (2) LPS (0.50 μg/mL, positive control); (3) Pepsin/trypsin mixture without MDP (1.00 mg/mL, enzyme control); (4) Complete medium alone (negative control). All treatment groups were incubated for 24 h at 37 °C in a 5% CO_2 humidified atmosphere.

2.13. Phagocytic assay

Phagocytic activity was assessed following Meng et al.[17] with modifications. MDP-treated RAW264.7 cells from Section 2.10 were collected and incubated with 100.00 μL FITC-labeled 40 kDa dextran (1 mg/mL) for 30 min at 37 °C. The reaction was terminated with 2.00 mL ice-cold PBS (pH 7.4), followed by three washes (300 × *g*, 5 min, 4 °C) with cold PBS. Cell suspensions were prepared in 400.00 μL of FACS buffer prior to analysis using a Beckman Coulter CytoFLEX Flow Cytometer (Brea, CA, USA) with excitation/emission at 488/525 nm, collecting 10,000 events per sample with appropriate gating strategies. Each sample was analyzed in six replicates.

2.14. Nitric oxide (NO), TNF-α and IL-6 production

After 24 h treatment (Section 2.10), cell supernatants were collected for NO, TNF-α, and IL-6 quantification using commercial kits per manufacturers' protocols, with quadruplicate measurements per sample.

2.15. Flow cytometry analysis

Surface marker expression was analyzed by flow cytometry following Sun et al.[18] with modifications. Briefly, treated cells were washed with ice-cold PBS and stained with 0.50 μg FITC Plus Anti-Mouse CD80 (16-10A1) or 0.25 μg FITC Plus Anti-Mouse CD86 (GL1) in 100.00 μL FACS buffer at room temperature (25 ± 2 °C) in the dark for 20 min. Cell suspensions were prepared in 400.00 μL L of FACS buffer prior to analysis using a Beckman Coulter CytoFLEX Flow Cytometer (Brea, CA, USA) with excitation/emission at 488/525 nm, collecting 10,000 events per sample with appropriate gating strategies. Each sample was analyzed in six replicates.

2.16. Statistical analysis

FlowJo version 10.8.1 (BD Biosciences, Franklin Lakes, NJ, USA) was utilized for flow cytometry data analysis. GraphPad Prism 8.0.2 (San Diego, CA, USA) served for statistical analysis, where one-way ANOVA established significance using these criteria: ns ($P > 0.05$), * ($P < 0.05$), ** ($P < 0.01$), *** ($P < 0.001$), and **** ($P < 0.0001$). OriginPro 2021 (OriginLab Corporation, Northampton, MA, USA) was employed for correlation analysis.

3. Results and discussion

3.1. Effect of aging duration on dried abalone quality

Color, as a critical quality attribute of dried aquatic products, profoundly influences their market value. Figure 1A displays dried abalone samples and their powders with various aging stages (0, 3, 5, and 10 years).

As demonstrated in Figure 1B, a gradual decrease in lightness (L^*) and whiteness (W^*) was observed with increasing aging time, indicating progressive browning during storage. It has been reported that the color changes are associated with Maillard reaction, which involves carbonyl-amine condensation between reducing sugars and amino acids, leading to the formation of melanoidins[19]. The browning intensity was quantitatively characterized by measuring absorbance at 294 nm and 420 nm (Figure 1C, D), serving as robust spectral markers for advanced glycation end-products[6]. The A_{294} increased from 0.53 to 0.93, while the A_{420} increased from 0.08 to 0.17, indicating substantial accumulation of browning-related compounds during the aging process. This chromatic trend aligns with observation in ready-to-eat abalone subjected to accelerated storage at 40 °C for 8 weeks, where a color shift from white to reddish-brown was attributed to the combined effects of the Maillard reaction and lipid oxidation[20]. However, the 3-year-aged dried abalone samples exhibited a deviation from the expected pattern, with reduced absorbance values and delayed browning kinetics, potentially attributable to the large size of 3-year-aged samples (~ 67.00 g/individual) compared to 0-year-aged controls (~ 45.00 g/individual), which resulted in reduced Maillard reaction-mediated browning in the internal muscle tissues.

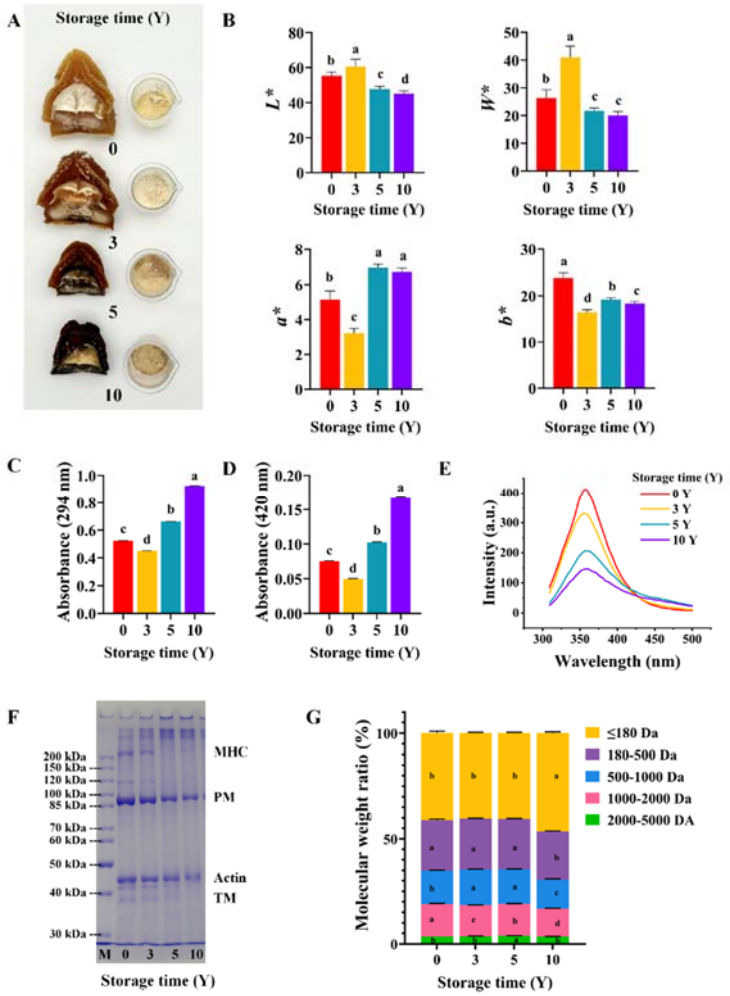

Figure 1. Physicochemical property evolution of dried abalone during aging. (A) Representative images of dried abalone samples and corresponding powders at various aging periods; (B) Color; (C) UV absorbance at 294 nm; (D) UV absorbance at 420 nm; (E) Intrinsic fluorescence spectra; (F) SDS-PAGE; (G) Molecular weight distribution ratios of dried abalone MDP. L^*: lightness; W^*: whiteness index; a^*: red-green chromaticity; b^*: yellow-blue chromaticity; MHC: myosin heavy chain; PM: paramyosin; TM: tropomyosin. Values with different lowercase letters as superscripts are significantly different at $P < 0.05$.

Fluorescence spectroscopic analysis revealed a time-dependent attenuation of intrinsic protein fluorescence intensity (Figure 1E), quantitatively reflecting the progressive accumulation of advanced glycation end-products (AGEs) during aging[15]. The observed inverse correlation between fluorescence intensity and glycation extent substantiates the occurrence of intermolecular fluorescence quenching mechanisms during protein-sugar conjugation[21]. Supporting SDS-PAGE profiles (Figure 1F) revealed a coordinated depletion of myofibrillar protein bands (myosin heavy chain, paramyosin, actin, and tropomyosin) concurrent with high-molecular-weight aggregate formation, unequivocally confirming the cooperative action of glycation and Maillard polymerization in driving covalent cross-linking[22]. These results demonstrate that dried abalone undergoes substantial browning reaction progression during extended ambient-temperature aging.

3.2. Molecular weight distribution and amino acid composition of MDP

Gel permeation chromatography (GPC) analysis revealed that the proportion of oligopeptides (<1000 Da) in MDP gradually increased with prolonged aging duration of dried abalone, reaching its peak in the MDP from 10-year-aged dried abalone (Figure 1G). This increase may be attributed to the Maillard reaction enhancing the susceptibility of proteins to pepsin digestion[23, 24], thereby facilitating the generation of oligopeptides. Studies have shown that oligopeptides under 1 kDa from *Lophius litulon* roe can activate immunosuppressed mouse models induced by cyclophosphamide, while similarly sized oligopeptides from *Stolephorus chinensis* promote the proliferation of RAW264.7 cells[25, 26]. Therefore, prolonged aging may improve the digestibility of dried abalone, leading to an increased yield of small oligopeptides with immunoregulatory potential.

The amino acid composition of MDP from dried abalone during various aging durations is summarized in Table 1. Glutamic acid (Glu) showed the most abundant amino acid, followed by arginine (Arg) and aspartic acid (Asp) as the subsequent predominant amino acids. The functional properties of immunomodulatory proteins or bioactive peptides are fundamentally governed by their amino acid composition, sequence characteristics, molecular chain length, and hydrophobicity[27]. Notably, positively charged amino acid residues such as Arg have been identified as recognition motifs for immunocyte receptors, directly involved in immune regulation[28]. This finding is corroborated by multiple studies as Ren et al.[25] have isolated low-molecular-weight bioactive peptides enriched with Arg, Glu, and Ser from *Lophius litulon* roe, while Ali et al.[28] have identified characteristic amino acid components (Ala, Asp, Gly, Glu, Ile, Pro, and Leu) in octopus peptide hydrolysates. These results suggest that the amino acid composition of dried abalone MDP may affect its immunomodulatory capacity.

Table 1 Effect of aging duration on amino acid content (g/100 g dry basis) of MDP

Amino acid	Storage time (Y)			
	0	**3**	**5**	**10**
Aspartic acid (Asp)	3.09±0.05^{c}	3.73±0.08^{a}	3.28±0.04^{b}	2.98±0.01^{d}
Glutamic acid (Glu)	5.32±0.14^{c}	6.45±0.11^{a}	5.67±0.08^{b}	5.05±0.00^{d}
Serine (Ser)	1.85±0.02^{c}	2.20±0.01^{a}	1.97±0.02^{b}	1.78±0.01^{d}
Histidine (His)	1.47±0.02^{a}	1.46±0.05^{a}	1.52±0.09^{a}	1.60±0.10^{a}

Glycine (Gly)	2.49±0.23^{c}	3.18±0.13^{a}	2.89±0.13^{b}	2.56±0.09^{c}
Threonine (Thr)	1.77±0.06^{c}	2.08±0.24^{a}	1.85±0.07^{ab}	1.79±0.01^{c}
Arginine (Arg)	3.22±0.11^{b}	3.77±0.07^{a}	3.81±0.03^{a}	3.13±0.01^{b}
Alanine (Ala)	2.08±0.70^{a}	1.76±0.04^{a}	2.22±0.19^{a}	1.69±0.01^{a}
Tyrosine (Tyr)	1.61±0.01^{c}	1.71±0.01^{b}	1.71±0.02^{b}	1.78±0.07^{a}
Cysteine (Cys)	1.91±0.00^{b}	1.91±0.05^{b}	1.93±0.09^{b}	2.26±0.26^{a}
Valine (Val)	1.27±0.02^{b}	1.50±0.01^{a}	1.33±0.05^{b}	1.04±0.10^{c}
Methionine (Met)	0.99±0.07^{c}	1.28±0.01^{a}	1.12±0.05^{b}	0.94±0.05^{c}
Phenylalanine (Phe)	1.98±0.10^{b}	2.14±0.08^{a}	1.47±0.01^{c}	1.35±0.02^{d}
Isoleucine (Ile)	1.01±0.03^{c}	1.00±0.03^{c}	1.68±0.01^{a}	1.60±0.03^{b}
Leucine (Leu)	2.44±0.07^{c}	2.85±0.02^{a}	2.62±0.05^{b}	2.32±0.02^{d}
Lysine (Lys)	1.85±0.36^{a}	1.81±0.49^{a}	2.30±0.29^{a}	1.62±0.22^{a}
Hydroxyproline (Hyp)	2.51±0.38^{a}	2.61±0.70^{a}	2.27±0.13^{a}	2.26±0.02^{a}
Proline (Pro)	1.78±0.04^{c}	2.12±0.12^{b}	2.55±0.20^{a}	2.40±0.05^{a}
Total amino acids	38.62±0.16^{c}	43.54±0.68^{a}	42.21±0.36^{b}	38.13±0.35^{c}
Hydrophobic amino acid	14.04±0.45^{b}	15.82±0.12^{a}	15.89±0.07^{a}	13.88±0.24^{b}
Umami amino acids	8.41±0.18^{c}	10.18±0.18^{a}	8.95±0.11^{b}	8.03±0.01^{d}
Sweet amino acids	9.97±0.46^{b}	11.34±0.24^{a}	11.48±0.22^{a}	10.22±0.07^{b}
Bitter amino acids	15.83±0.56^{b}	17.50±0.42^{a}	17.57±0.23^{a}	15.36±0.39^{b}

Hydrophobic amino acid: Gly, Ala, Val, Met, Phe, Ile, Leu, and Pro.
Umami amino acids: Asp and Glu.
Sweet amino acids: Thr, Ser, Pro, Gly, and Ala.
Bitter amino acids: Val, Met, Leu, Ile, Tyr, Phe, His, Lys, and Arg.
Data are expressed as mean ± standard deviation (n = 3).
Samples with different lowercase letters (a-d) indicate significant differences ($P < 0.05$).

3.3. Effects of MDP on proliferation and phagocytic activity of RAW264.7 cells

As shown in Figure 2A, cell proliferation was significantly enhanced by 24-h MDP treatment ($P < 0.05$). The highest concentration (12.80 mg/mL) was found to exhibit a relatively lower proliferative effect when compared to optimal concentrations. Consequently, the concentration of 0.10-6.40 mg/mL range was selected for subsequent experimental evaluation. Concentration-dependent proliferation was observed, and optimal activity was achieved at 6.40 mg/mL. The most potent proliferative effect was demonstrated by the 3-year-aged dried abalone MDP at this concentration, achieving a proliferation rate of 236.37% relative to control. Notably, MDP co-treatment with LPS further enhanced proliferation (Figure 2B), suggesting potential adjuvant-like immunostimulatory effects.

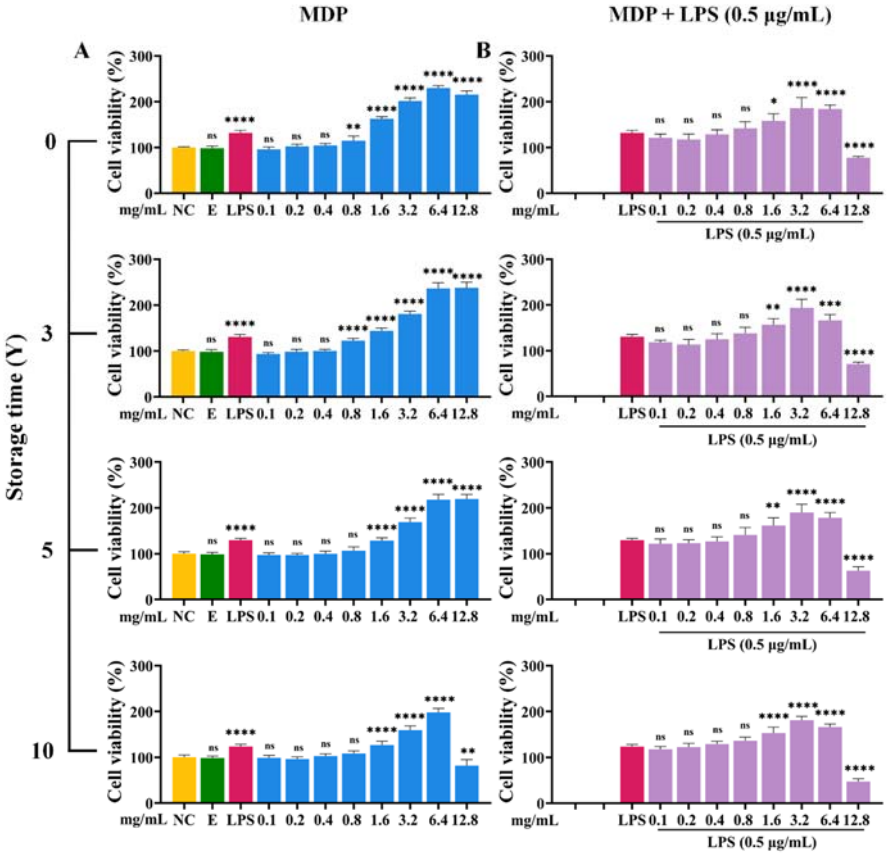

Figure 2. Effects of MDP from dried abalone of different storage durations on cell proliferation in RAW264.7 cells. (A) Cell viability of MDP-treated cells without LPS; (B) Cell viability of MDP-treated cells with LPS. NC: Negative control; E: Enzyme control.

Phagocytic assay results (Figure 3A-C) demonstrated that MDP treatment for 24 h significantly enhanced particle uptake regardless of LPS co-stimulation ($P < 0.05$). Maximal phagocytic activity of 42.79% was induced by treatment with 6.40 mg/mL of 0-year-aged dried abalone MDP in the absence of LPS stimulation, while peak phagocytosis of 79.50% was achieved through LPS co-stimulation with 6.40 mg/mL of 3-year-aged dried abalone MDP. These findings carry significant immunological implications, given that macrophage proliferation and phagocytosis are critical for innate immune defense, essential for pathogen clearance and antigen presentation. The observed proliferative effects are similar to previous reports on immunomodulatory peptides from silkworm pupae[29], tilapia hydrolysates[30], and *Quasipaa spinosa*[12], while phagocytic enhancement parallels findings in selenium-containing peptides studies[31]. Notably, casein glycopeptide O-glycans (B-GMP) induced stronger proliferation of 147.00% at 25.00 μg/mL, due to their immunoreactive glycan moieties[32]. This implies that glycosylated products accumulated during abalone's prolonged aging process could potentially enhance MDP's immunostimulatory effects via analogous carbohydrate-dependent pathways.

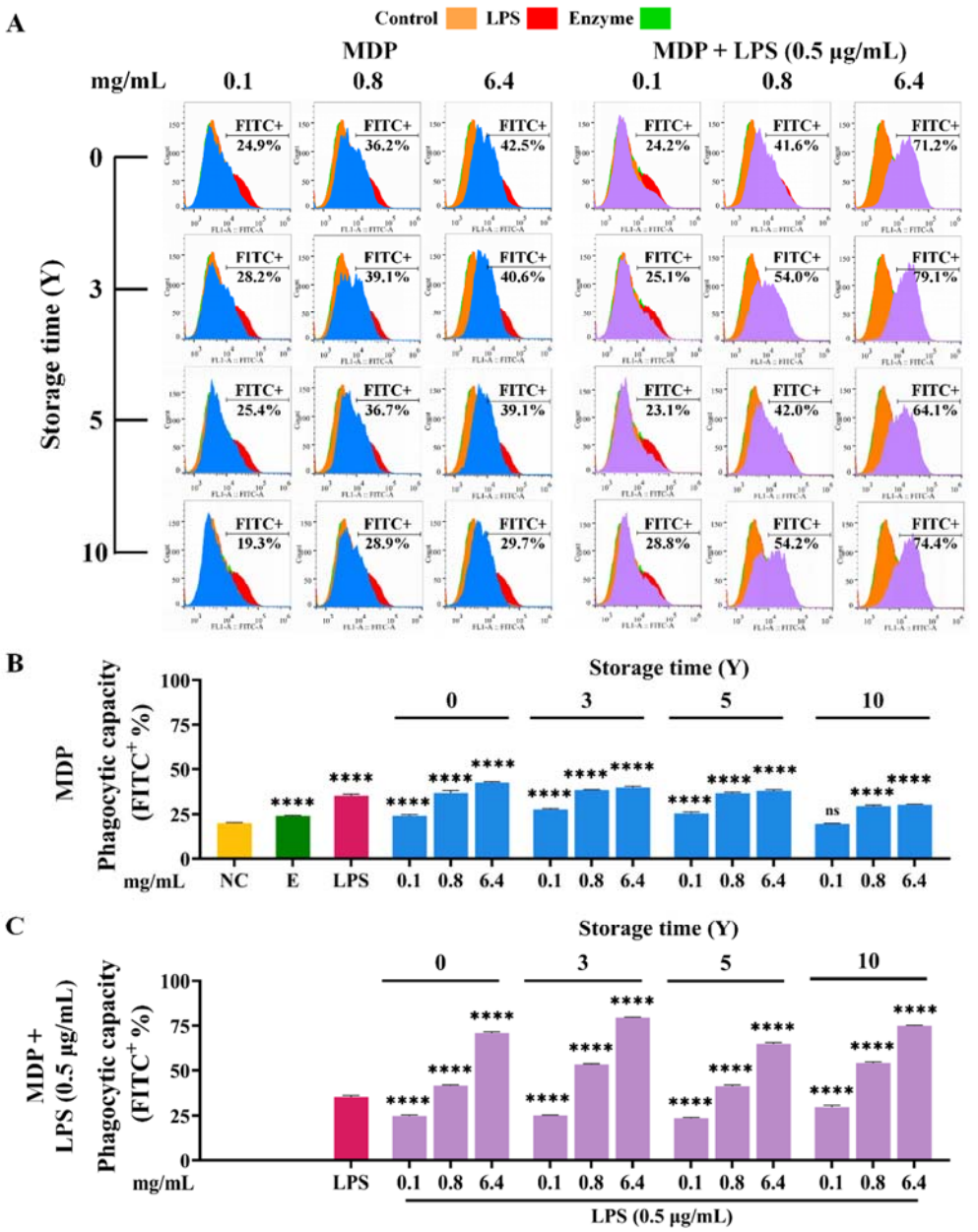

Figure 3. Effects of MDP from dried abalone of different durations on macrophage phagocytosis in RAW264.7 cells. (A) Percentage of FITC+ cells; (B) Phagocytic capacity of MDP-treated cells without LPS stimulation; (C) Phagocytic capacity of MDP-treated cells with LPS. NC: Negative control; E: Enzyme control.

3.4. Effects of MDP on NO and cytokine secretion in RAW264.7 cells

Nitric oxide (NO), an important biological mediator, contributes significantly to innate immune defense by participating in critical processes including microbial eradication, maintenance of immune balance, and wound healing, with its production primarily dependent on macrophage activation[33]. As shown in Figures 4A and B, MDP treatment for 24 h significantly enhanced NO production in RAW264.7 cells, regardless of LPS stimulation ($P < 0.05$). Treatment with 6.40 mg/mL of 0-year-aged dried abalone MDP induced maximal NO secretion of 1.53 μM. This observation aligns well with previous reports on the concentration-dependent NO induction by ≤3 kDa coix seed hydrolysates[34] and the iNOS-upregulating properties of a novel pentadecapeptide from *Cyclina sinensis*[35].

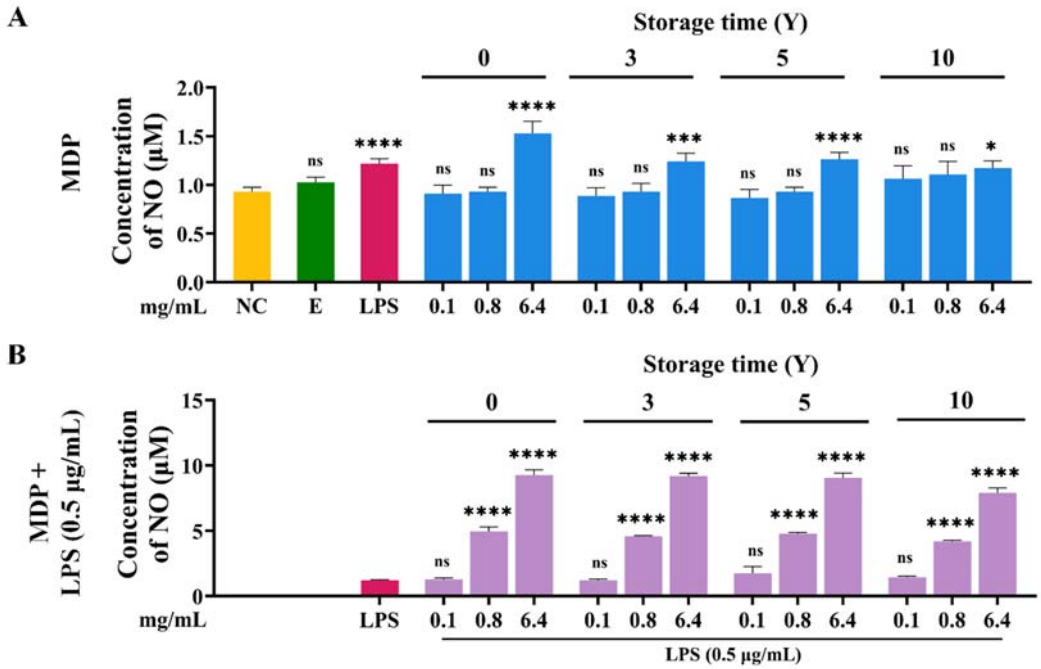

Figure 4. Effects of MDP from dried abalone of different durations on NO secretion in RAW264.7 cells. (A) Basal NO secretion without LPS stimulation; (B) LPS-induced NO secretion. NC: Negative control; E: Enzyme control.

Cytokines represent fundamental molecular messengers in immunological networks, being responsible for immune modulation, intracellular signaling, and inflammation regulation[36]. TNF-α and IL-6 are particularly note for their contributions to macrophage functional activation and antigen processing, while also being involved in mediating crosstalk between innate and adaptive immune systems through multiple biological mechanisms[37]. As shown in Figure 5A and B, distinct modulation patterns of TNF-α secretion were observed in RAW264.7 cells following 24 h MDP treatment ($P < 0.05$). Under LPS-free conditions, the strongest immunostimulatory activity was demonstrated by 0-year-aged dried abalone MDP at 6.40 mg/mL, with TNF-α secretion induced up to 19.18 ng/mL. In contrast, under LPS co-stimulation, maximal immunoadjuvant effect was shown by 5-year-aged dried abalone MDP at 6.40 mg/mL, resulting in TNF-α production being elevated from 45.50 to 122.89 ng/mL and representing a 2.70-fold increase compared to LPS stimulation alone. As shown in Figure 5C and D, IL-6 secretion was found to be strictly LPS-dependence. Although no detectable IL-6 release was stimulated by MDP alone, significant enhancement was observed in LPS-primed cells. The most potent immunoadjuvant activity was exhibited by 5-year-aged dried abalone MDP at 0.80 mg/mL, with IL-6 production being boosting from 5.72 to 19.52 ng/mL, which was 3.41-fold higher than that induced by LPS alone. These results collectively indicate that MDP from dried abalone aged for different durations exhibited distinct cytokine modulation profiles: 0-year-aged dried abalone MDP exhibited stronger direct immunostimulatory capacity, while 5-year-aged dried abalone MDPs showed superior immunoadjuvant effects when combined with LPS. These observations align with previous reports on immunomodulatory peptides derived from soybean[38], *Mytilus coruscu*[39], and duck egg ovalbumin[40], but found the previously overlooked adjuvant-like potential of dietary peptides. Immune adjuvants enhance adaptive immunity by promoting antigen-presenting cell (APC) maturation and activation via induction of pro-inflammatory cytokines[41], which is consistent with our findings.

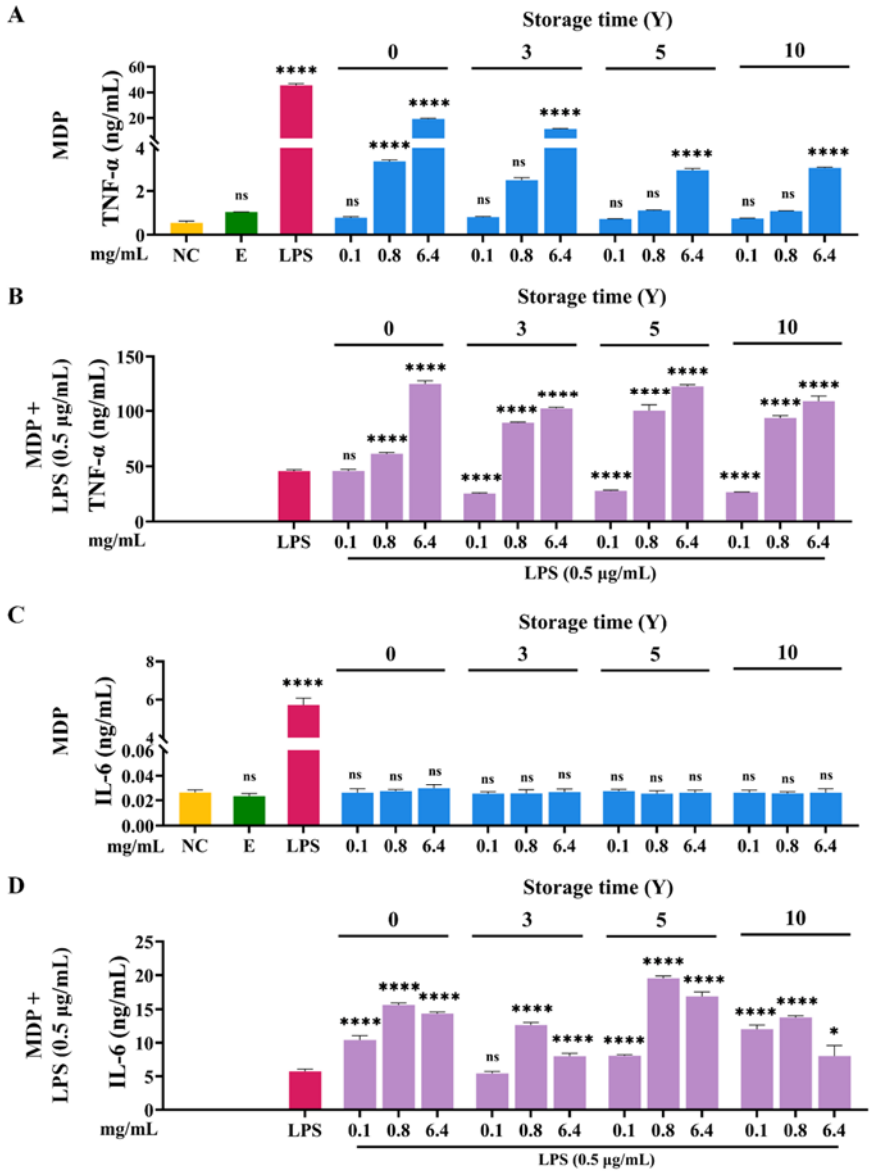

Figure 5. Effects of MDP from dried abalone of different durations on pro-inflammatory cytokine secretion in RAW264.7 cells. (A) Basal TNF-α production without LPS stimulation; (B) LPS-stimulated TNF-α production; (C) Basal IL-6 secretion without LPS; (D) LPS-induced IL-6 secretion. NC: Negative control; E: Enzyme control.

3.5. Effects of MDP on expression of co-stimulatory molecules CD80 and CD86 on RAW264.7 cells

As professional APC, macrophages activate T-cell responses via the CD80/CD86-CD28 co-stimulatory pathway, providing critical secondary signals for T-cell activation[42]. Regarding CD80 expression, the highest CD80 expression was observed with 3-year-aged dried abalone MDP at 6.40 mg/mL under LPS-free conditions, increasing positive cells from a baseline of 1.60% to 5.05%. When co-administered with LPS, the most pronounced immunoadjuvant effect was produced by 5-year-aged dried abalone MDP at 0.80 mg/mL, elevating CD80-positive cells to 94.22% compared to 7.41% with LPS alone (Figure 6A-C). For CD86 expression, maximal enhancement was achieved by 3-year-aged dried abalone MDP at 0.80 mg/mL in the absence of LPS stimulation, increasing positive cells from 11.90% to 13.33%. Under LPS co-stimulation, the strongest enhancement was achieved by 5-year-aged dried abalone MDP at 0.10 mg/mL, which raised CD86-positive cells to 68.87% versus 51.30% with LPS alone (Figure 7A-C). Of particular note was the

observation that reduced CD86 expression was exhibited by all MDP samples at higher concentrations, suggesting the induction of immune tolerance by MDP at elevated concentrations. The differential regulation patterns between CD80 and CD86 likely reflect their temporal expression kinetics during immune responses-CD86 typically responds rapidly in early activation phases, while CD80 expression peaks later during sustained stimulation[43]. The observed co-stimulatory molecule induction aligns with mechanisms of classical immune adjuvants. For instance, aluminum adjuvants enhance CD80/CD86 expression on dendritic cells through caspase-1-dependent pathways[44]. In addition, several previous studies have reported similar immunomodulatory effects mediated through different molecular pathways. *Escherichia coli* maltose-binding protein could upregulate CD80 expression in RAW264.7 macrophages via TLR2/TLR4-dependent mechanisms[45]; and *Cirsii Herba* glycoproteins induce M1 polarization through TLR4-mediated activation of MAPK and NF-κB signaling cascades[46]. These results demonstrate that MDP effectively promote CD80/CD86 expression in RAW264.7 macrophages. However, the precise intracellular signaling pathways involved require further investigation.

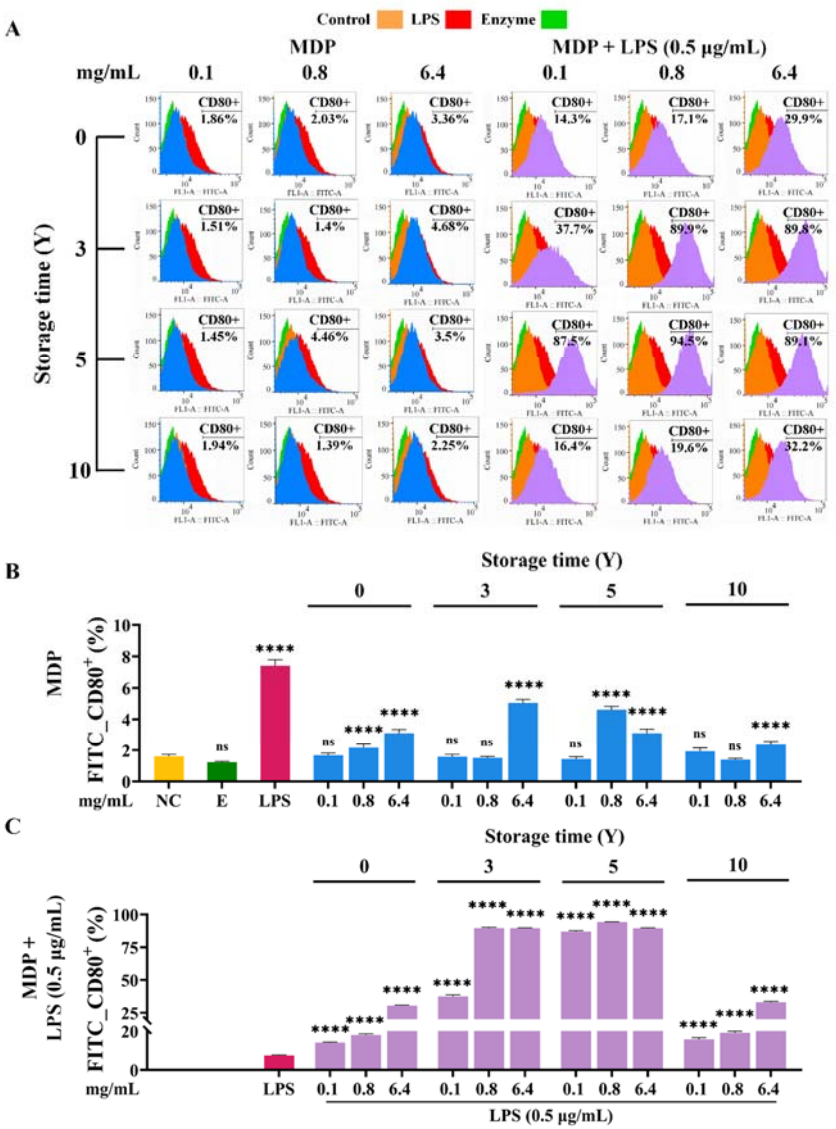

Figure 6. Effects of MDP from dried abalone of different durations on CD80 expression in RAW264.7 cells. (A) Percentage of CD80+ cells; (B) Baseline CD80 expression without LPS; (C) LPS-induced CD80 expression. NC: Negative control; E: Enzyme control.

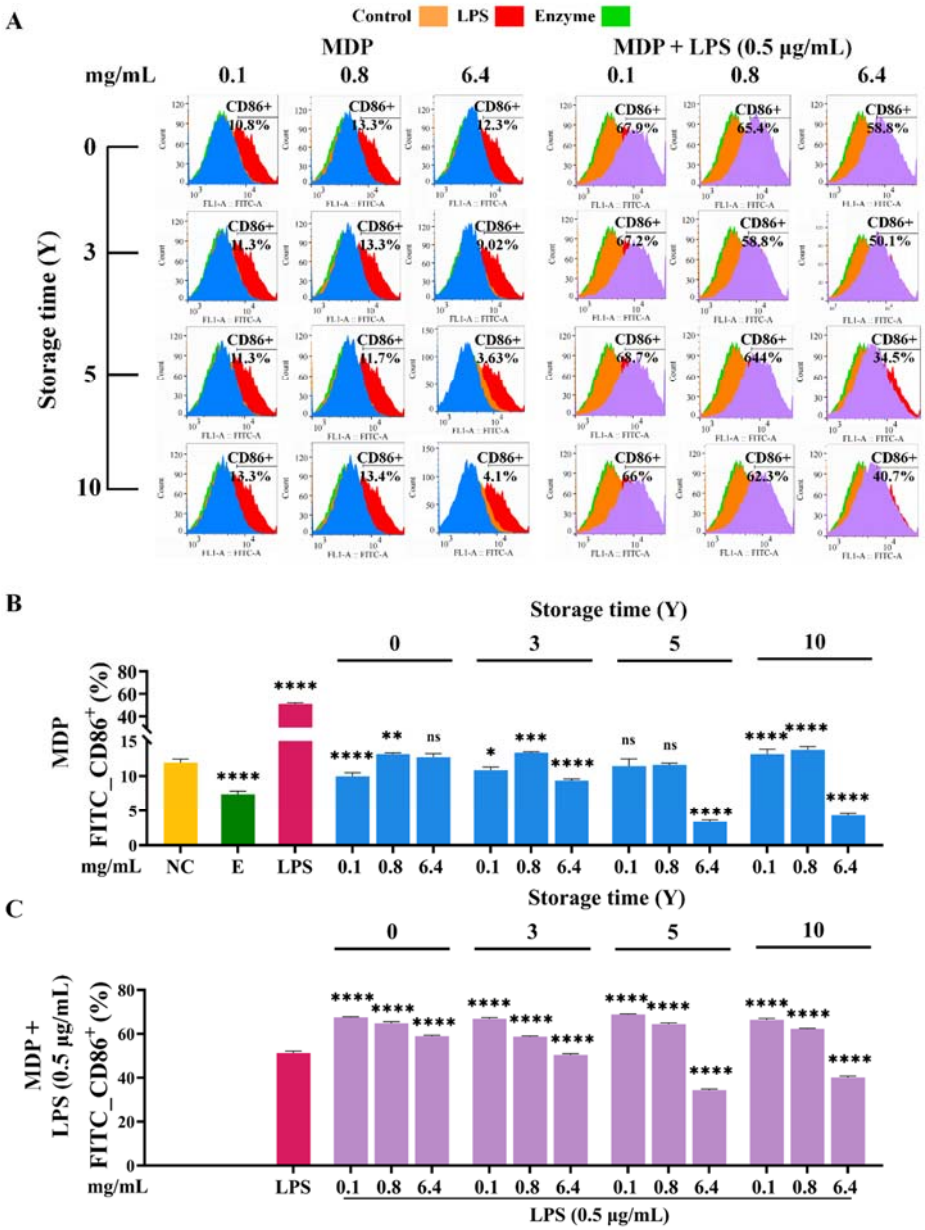

Figure 7. Effects of MDP from dried abalone of different durations on CD86 expression in RAW264.7 cells. (A) Percentage of CD86+ cells; (B) Baseline CD86 expression without LPS; (C) LPS-induced CD86 expression. NC: Negative control; E: Enzyme control.

3.6 General discussion

During long-term storage, the Maillard reaction occurs in food products[47], which may enhance the susceptibility of proteins to pepsin[23,24]. As a result, 10-year-aged dried abalone was more easily digested by pepsin-trypsin to generate oligopeptides (Figure 1G). However, the 5-year-aged dried abalone MDP exhibited the strongest immunomodulatory activity, whereas the activity of the 10-year-aged dried abalone MDP was somewhat reduced. Correlation analysis revealed that, in the presence of LPS, the expression levels of CD80 and CD86 on the cell surface were positively correlated with the proportion of 180-1000 Da oligopeptides in MDP, but negatively correlated with the proportion of components ≤180 Da (Figure 8). This suggests that the oligopeptide components in MDP possess immunoadjuvant effects, whereas an increase in small molecular components ≤180 Da may reduce the activity. Generally, the immunomodulatory capacity of peptides is

related to their molecular weight and amino acid composition[48], and free amino acids basically lack bioactivity[49]. Among immunomodulatory peptides, hydrophobic amino acids, Glu, and Arg are the most common residues[48]. In this study, compared to other MDP samples, the 5-year-aged dried abalone MDP had higher contents of Arg, Glu, and hydrophobic amino acids (Table 1), which may have enhanced its ability to bind receptors on the surface of immune cell, thereby enhancing immunomodulatory activity[28]. Therefore, the Maillard reaction promoted proteolytic digestion of dried abalone during aging, leading to oligopeptide generation. The MDP from 5-year-aged dried abalone showed the strongest immunoadjuvant effect, likely due to its richness in immunomodulatory oligopeptides within 180-1000 Da range and its higher content of key amino acids. Future research will focus on the isolation, purification, and characterization of immunomodulatory oligopeptides in the 180-1000 Da fraction.

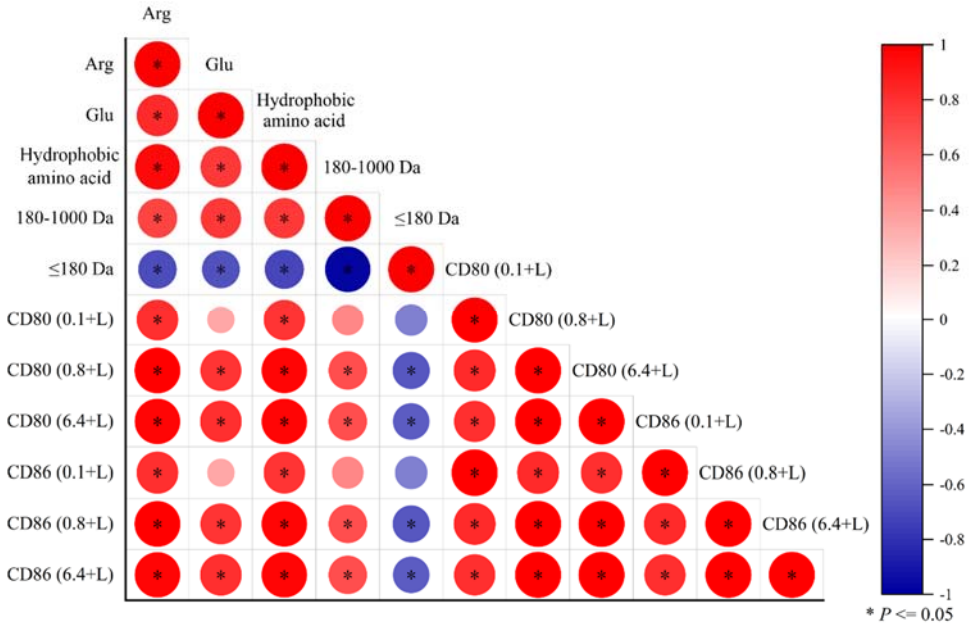

Figure 8. Correlation of the effect of dried abalone MDP on CD80 and CD86 expression in RAW264.7 cells with its molecular weight and key amino acid content in the presence of LPS.

4. Conclusions

This study elucidated the progression of the Maillard reaction in dried abalone during a 10-year aging duration at ambient temperature, as well as its impact on the immunomodulatory activity of dried abalone MDP. The results demonstrated that aging not only promoted protein cross-linking and aggregation induced by the Maillard reaction, but also led to an increase in oligopeptides smaller than 1 kDa after simulated digestion of dried abalone. In the presence of LPS, 5-year-aged dried abalone MDP significantly upregulated the secretion of TNF-α, IL-6 and the expression of CD80/CD86 in RAW264.7 cells, demonstrating the strongest immunoadjuvant effect. In contrast, a notable reduction in activity was observed with the 10-year-aged dried abalone MDP. Analysis indicated that excessive aging may result in an overly high proportion of components below 180 Da in the dried abalone MDP, along with depletion of immunologically relevant amino acids. These findings clarify the impact of long-term natural aging on the immunomodulatory potential of dried abalone, providing a scientific basis for understanding the functional and nutritional value of

traditionally aged dried abalone. Further research will focus on isolating and identifying oligopeptides and glycopeptides from the dried abalone MDP, with their immunomodulatory efficacy and mechanisms being further verified using animal experiments and molecular biology techniques.

Declaration of competing interest

The authors declare that they have no known competing financial interests or personal relationships that could have appeared to influence the work reported in this paper.

Acknowledgments

This work is sponsored by Major Science and Technology Special Project of Fujian Province (2024NZ031015) and Xiamen Science and Technology Project (2022CXY0312).

References

[1] V. Venugopal, K. Gopakumar, Shellfish: Nutritive value, health benefits, and consumer safety, Compr. Rev. Food. Sci. Food Saf. 16 (2017) 1219-1242. https://doi.org/10.1111/1541-4337.12312.

[2] L. Shi, G. Hao, J. Chen, et al., Nutritional evaluation of Japanese abalone (*Haliotis discus hannai Ino*) muscle: Mineral content, amino acid profile and protein digestibility, Food Res. Int. 129 (2020) 108876. https://doi.org/https://doi.org/10.1016/j.foodres.2019.108876.

[3] Anonymous, China fishery statistical yearbook, China Agriculture Press, Beijing, 2024.

[4] J. Zeng, Y. Song, P. Cong, et al., A systematic review of drying in aquatic products, Rev. Aquac. 16 (2024) 47-65. https://doi.org/https://doi.org/10.1111/raq.12820.

[5] Y. Mo, J. Ma, X. Zhang, et al., Peptide gelation contributes to the tenderness and viscoelasticity of candy abalone, Eur. Food Res. Technol. 250 (2024) 1865-1879. https://doi.org/10.1007/s00217-024-04523-x.

[6] Y. Luo, X.-B. Zeng, Y.-Y. Hu, et al., Differences and mechanisms of color deterioration in three types of ready-to-eat shellfishes during storage, Food Chem. 469 (2025) 142459. https://doi.org/https://doi.org/10.1016/j.foodchem.2024.142459.

[7] Tian Y, You S, Zhang Y, et al. Proteomic studies of the effects of processing techniques on properties of abalone muscles: A comprehensive review. Food Sci. Human Wellness (2024) 9250254. https://doi.org/10.26599/FSHW.2024.9250254.

[8] S.H. Chun, K.W. Lee, Immune-enhancing effects of β-lactoglobulin glycated with lactose following *in vitro* digestion on cyclophosphamide-induced immunosuppressed mice, J. Dairy Sci. 105 (2022) 623-636. https://doi.org/10.3168/jds.2021-20681.

[9] Shi L, Hao G, Chen J, et al. Structural characterization and immunostimulatory activity of a water-soluble polysaccharide from abalone (*Haliotis discus hannai Ino*) muscle. Food Sci. Human Wellness 12 (2023) 495-502. https://doi.org/10.1016/j.fshw.2022.07.051.

[10] H.A.R. Suleria, R. Addepalli, P. Masci, et al., *In vitro* anti-inflammatory activities of blacklip abalone (*Haliotis rubra*) in RAW 264.7 macrophages, Food Agric. Immunol. 28 (2017) 711-724. https://doi.org/10.1080/09540105.2017.1310186.

[11] P. He, L. Pan, H. Wu, et al., Isolation, identification, and immunomodulatory mechanism of peptides from *Lepidium meyenii* (Maca) protein hydrolysate, J. Agric. Food Chem. 70 (2022) 4328-4341. https://doi.org/10.1021/acs.jafc.1c08315.

[12] Y. Zeng, H. Cheng, R. Zhong, et al., Novel immunomodulatory peptides from hydrolysates of the Rana spinosa (*Quasipaa spinosa*) meat and their immunomodulatory activity mechanism, Food Chem. 465 (2025) 142024. https://doi.org/https://doi.org/10.1016/j.foodchem.2024.142024.

[13] U.K. Laemmli, Cleavage of structural proteins during the assembly of the head of bacteriophage T4, Nature 227 (1970) 680-685. https://pubmed.ncbi.nlm.nih.gov/5432063.

[14] Y. Luo, X. Zeng, Y. Hu, et al., Differences and mechanisms of color deterioration in three types of ready-to-eat shellfishes during storage, Food Chem. 469 (2025) 142459. https://doi.org/https://doi.org/10.1016/j.foodchem.2024.142459.

[15] J. Qiu, Q. Zheng, L. Fang, et al., Preparation and characterization of casein-carrageenan conjugates and self-assembled microcapsules for encapsulation of red pigment from paprika, Carbohydr. Polym. 196 (2018) 322-331. https://doi.org/10.1016/j.carbpol.2018.05.054.

[16] W. Weng, L. Tang, B. Wang, et al., Antioxidant properties of fractions isolated from blue shark (*Prionace glauca*) skin gelatin hydrolysates, J. Funct. Food. 11 (2014) 342-351. https://doi.org/https://doi.org/10.1016/j.jff.2014.10.021.

[17] L. Meng, K. Feng, L. Wang, et al., Activation of mouse macrophages and dendritic cells induced by polysaccharides from a novel *Cordyceps sinensis* fungus UM01, J. Funct. Food. 9 (2014) 242-253. https://doi.org/https://doi.org/10.1016/j.jff.2014.04.029.

[18] H. Sun, J. Zhang, F. Chen, et al., Activation of RAW264.7 macrophages by the polysaccharide from the roots of *Actinidia eriantha* and its molecular mechanisms, Carbohydr. Polym. 121 (2015) 388-402. https://doi.org/10.1016/j.carbpol.2014.12.023.

[19] D. Kathuria, Hamid, S. Gautam, et al., Maillard reaction in different food products: Effect on product quality, human health and mitigation strategies, Food Control 153 (2023) 109911. https://doi.org/https://doi.org/10.1016/j.foodcont.2023.109911.

[20] Y. Fan, M. Yu, D. Li, et al., Effects of non-enzymatic browning and lipid oxidation on color of ready-to-eat abalone during accelerated storage and its control, Foods 12 (2023) 1514. https://www.mdpi.com/2304-8158/12/7/1514.

[21] Y. Zheng, Y. Chang, B. Luo, et al., Molecular structure modification of ovalbumin through controlled glycosylation with dextran for its emulsibility improvement, Int. J. Biol. Macromol. 194 (2022) 1-8. https://doi.org/https://doi.org/10.1016/j.ijbiomac.2021.11.130.

[22] B. Chen, L. Chen, C. Li, et al., Ultrasound-assisted glycosylation of ovalbumin and dextran conjugate carrier for anthocyanins and their stability evaluation, Ultrason. Sonochem. 109 (2024) 107024. https://doi.org/https://doi.org/10.1016/j.ultsonch.2024.107024.

[23] Z. Li, Y. Luo, L. Feng, et al., Effect of Maillard reaction conditions on antigenicity of β-lactoglobulin and the properties of glycated whey protein during simulated gastric digestion. Food Agric. Immunol. 24 (2012) 433-443. https://doi.org/10.1080/09540105.2012.712951.

[24] Y. Joubran, A. Moscovici, R. Portmann, et al., Implications of the Maillard reaction on bovine alpha-lactalbumin and its proteolysis during *in vitro* infant digestion. Food Funct. 8 (2017) 2295-2308. https://doi.org/10.1039/c7fo00588a.

[25] Z. Ren, F. Yang, S. Yao, et al., Effects of low molecular weight peptides from monkfish (*Lophius litulon*) roe on immune response in immunosuppressed mice, Front. Nutr. 9 (2022) 929105. https://doi.org/10.3389/fnut.2022.929105.

[26] B. Xu, L. Ye, Y. Tang, et al., Preparation and purification of an immunoregulatory peptide from *Stolephorus chinensis* of the East Sea of China, Process Biochem. 98 (2020) 151-159. https://doi.org/https://doi.org/10.1016/j.procbio.2020.08.011.

[27] H.K. Kang, H.H. Lee, C.H. Seo, et al., Antimicrobial and immunomodulatory properties and applications of marine-derived proteins and peptides, Mar. Drugs 17 (2019) 350. https://www.mdpi.com/1660-3397/17/6/350.

[28] M. Ali, H. Ullah, N.A. Farooqui, et al., NF-κB pathway activation by Octopus peptide hydrolysate ameliorates gut dysbiosis and enhances immune response in cyclophosphamide-induced mice, Heliyon 10 (2024) e38370. https://doi.org/10.1016/j.heliyon.2024.e38370.

[29] Y. Guo, M. Xu, X. Hu, et al., Extraction, purification, and mechanism of immunomodulatory peptides obtained from silkworm pupa protein hydrolysate, Int. J. Biol. Macromol. 283 (2024) 137863. https://doi.org/10.1016/j.ijbiomac.2024.137863.

[30] K. Liu, I.P. Kuo, Y. Chen, et al., Oral administration of tilapia hydrolysate peptides ameliorates the immune-related side effects of cyclophosphamide in BALB/c mice, Food Biosci. 56 (2023) 103428. https://doi.org/https://doi.org/10.1016/j.fbio.2023.103428.

[31] Y. Fang, X. Pan, E. Zhao, et al., Isolation and identification of immunomodulatory selenium-containing peptides from selenium-enriched rice protein hydrolysates, Food Chem. 275 (2019) 696-702. https://doi.org/https://doi.org/10.1016/j.foodchem.2018.09.115.

[32] Y. Lu, J. Liu, Z. Li, et al., Comparative mass spectrometry analysis and immunomodulatory effects of casein glycomacropeptide O-glycans in bovine and caprine whey powder, J. Agric. Food Chem. 70 (2022) 8746-8754. https://doi.org/10.1021/acs.jafc.1c07975.

[33] M.J. Sweet, D. Ramnath, A. Singhal, et al., Inducible antibacterial responses in macrophages, Nat. Rev. Immunol. 25 (2025) 92-107. https://doi.org/10.1038/s41577-024-01080-y.

[34] L. Li, B. Li, H. Ji, et al., Immunomodulatory activity of small molecular (≤3 kDa) *Coix glutelin* enzymatic hydrolysate, CyTA-J. Food 15 (2017) 41-48. https://doi.org/10.1080/19476337.2016.1201147.

[35] W. Li, S. Ye, Z. Zhang, et al., Purification and characterization of a novel pentadecapeptide from protein hydrolysates of *Cyclina sinensis* and its immunomodulatory effects on RAW264.7 cells, Mar. Drugs 17 (2019) 30. https://www.mdpi.com/1660-3397/17/1/30.

[36] A. Mantovani, C.A. Dinarello, M. Molgora, et al., Interleukin-1 and related cytokines in the regulation of inflammation and immunity, Immunity 50 (2019) 778-795. https://doi.org/10.1016/j.immuni.2019.03.012.

[37] B. Toledo, L. Zhu Chen, M. Paniagua-Sancho, et al., Deciphering the performance of macrophages in tumour microenvironment: a call for precision immunotherapy, J. Hematol. Oncol. 17 (2024) 44. https://doi.org/10.1186/s13045-024-01559-0.

[38] L. Wen, Y. Jiang, X. Zhou, et al., Structure identification of soybean peptides and their immunomodulatory activity, Food Chem. 359 (2021) 129970. https://doi.org/https://doi.org/10.1016/j.foodchem.2021.129970.

[39] K. He, Y. Zeng, H. Tian, et al., Macrophage immunomodulatory effects of low molecular weight peptides from *Mytilus coruscus* via NF-κB/MAPK signaling pathways, J. Funct. Food. 83 (2021) 104562. https://doi.org/https://doi.org/10.1016/j.jff.2021.104562.

[40] P. He, Q. Wang, Q. Zhan, et al., Purification and characterization of immunomodulatory peptides from enzymatic hydrolysates of duck egg ovalbumin, Food Funct. 12 (2021) 668-681. https://doi.org/10.1039/d0fo02674c.

[41] T. Zhao, Y. Cai, Y. Jiang, et al., Vaccine adjuvants: Mechanisms and platforms, Signal Transduct. Target. Ther. 8 (2023) 283. https://doi.org/10.1038/s41392-023-01557-7.

[42] L. Yan, J. Wang, X. Cai, et al., Macrophage plasticity: Signaling pathways, tissue repair, and regeneration, MedComm 5 (2024) e658. https://doi.org/10.1002/mco2.658.

[43] A.H. Sharpe, G.J. Freeman, The B7–CD28 superfamily, Nat. Rev. Immunol. 2 (2002) 116-126. https://doi.org/10.1038/nri727.

[44] A. Sokolovska, S.L. Hem, H. HogenEsch, Activation of dendritic cells and induction of CD4+ T cell differentiation by aluminum-containing adjuvants, Vaccine 25 (2007) 4575-4585. https://doi.org/https://doi.org/10.1016/j.vaccine.2007.03.045.

[45] W. Wang, H. Yuan, G. Liu, et al., *Escherichia coli* maltose-binding protein induces M1 polarity of RAW264.7 macrophage cells via a TLR2- and TLR4-dependent manner, Int. J. Mol. Sci. 16 (2015) 9896-9909. https://www.mdpi.com/1422-0067/16/5/9896.

[46] M. Zhao, S. Qin, J. Wang, et al., *Cirsii Herba* glycoprotein promotes macrophage M1 polarization through MAPK and NF-κB signaling pathways via interaction with TLR4, Int. J. Biol. Macromol. 296 (2025) 139687. https://doi.org/10.1016/j.ijbiomac.2025.139687.

[47] K. Arihara, I. Yokoyama, M. Ohata, Bioactivities generated from meat proteins by enzymatic hydrolysis and the Maillard reaction, Meat Sci. 180 (2021) 108561. https://doi.org/10.1016/j.meatsci.2021.108561.

[48] M. Chalamaiah, W. Yu, J. Wu, Immunomodulatory and anticancer protein hydrolysates (peptides) from food proteins: A review, Food Chem. 245 (2018) 205-222. https://doi.org/10.1016/j.foodchem.2017.10.087.

[49] M. Akbarian, A. Khani, S. Eghbalpour, V.N. Uversky, et al., Bioactive peptides: Synthesis, sources, applications, and proposed mechanisms of action, Int. J. Mol. Sci. 23 (2022) 1445. https://doi.org/10.3390/ijms23031445.